

## Supporting Information

MnO<sub>2</sub> nanoparticles as a minimalist multimode vaccine adjuvant/delivery system to regulate antigen presenting cells for tumor immunotherapy

Ting Song <sup>a,1</sup>, Yang Liao <sup>b,1</sup>, Qinhua Zuo <sup>a</sup>, Ning Liu <sup>c,\*</sup>, Zonghua Liu <sup>a,\*</sup>

<sup>a</sup> Department of Biomedical Engineering, Jinan University, Guangzhou, China, 510632

<sup>b</sup> Department of Laboratory Medicine, General Hospital of Southern Theatre Command of PLA, Guangzhou 510010, China

<sup>c</sup> Department of Bone and Joint Surgery, The First Affiliated Hospital, Jinan University, Guangzhou, China, 510632

Corresponding authors:

Zonghua Liu (tliuzonghua@jnu.edu.cn)

Ning Liu (liuning@163.com)

<sup>1</sup> These authors contributed equally to this work and should be considered co-first authors.

## **Measurement**

The Synthetic MnO<sub>2</sub> nanoparticles were examined with an X-ray diffractor (Miniflex 600, Rigaku, Japan). The  $\zeta$ -potential, hydrodynamic size distribution of MnO<sub>2</sub> were measured through the dynamic light scattering instrument (Nano ZS, Malvern). The Mn concentration in MnO<sub>2</sub> was determined by an inductively coupled plasma-mass spectroscopy (ICP-MS, Thermo iCAP 7000 AERIES, USA).

## **Colloidal stability measurement**

For the observation of colloid stabilization, 1mg/mL of MnO<sub>2</sub> were dispersed in DI water, PBS (10 mM, pH=7.4), saline, and RPMI-1640 culture medium respectively. Then the photos were taken to monitor the colloidal stability in 24 h. Furthermore, to test the stability of MnO<sub>2</sub> in water, PBS/pH7.4 solution, saline and 1640 medium solution, the particle size and zeta potential of the MnO<sub>2</sub> nanoparticles were measured by DLS at defined time points.

## **Slow release of Mn<sup>2+</sup> from MnO<sub>2</sub> in vitro**

The release of Mn<sup>2+</sup> from the MnO<sub>2</sub> nanoparticles in vitro was investigated. The MnO<sub>2</sub> was incubated with phosphate buffer solution (pH5.0 or 7.4), and the solution was centrifuged (10000 rpm, 20 min) at different time points. Then, the Mn<sup>2+</sup> in the supernatant was detected by ICP-MS. Then the photos were taken to monitor the stability in 7 days. Moreover, the Mn<sup>2+</sup> release from the MnO<sub>2</sub> nanoparticles (in PBS/pH7.4 or 5.0) were detected by ICP-MS (the aqueous solution group is the control).

## **In vitro cytotoxicity analysis**

The in vitro cytotoxicity of MnO<sub>2</sub> nanoparticles was detected by CCK-8 assay. Firstly, DC2.4, B16 and 4T1 cells were seeded in a 96-well plate at density of  $1 \times 10^4$  cells/well, respectively. After overnight incubation, the original medium was replaced with fresh complete medium containing MnO<sub>2</sub> with different concentration. Subsequently, the cells were incubated at 37°C for 24 h. After 24 h, the cells were washed with PBS, then, 100  $\mu$ L of fresh medium containing 10% CCK-8 was added to each well. The cells were incubated again for 20 minutes. Finally, the absorbance at 450 nm of each well was detected by a microplate reader (Cytation5, Biotek, USA).

### Detection of intracellular reactive oxygen species (ROS)

To detect intracellular ROS in vitro, briefly, DC2.4 cells were seeded into 6-well plates at a density of  $1 \times 10^5$  cells per well and incubated at  $37^\circ\text{C}$  overnight. Then, cells were treated with the  $\text{MnO}_2$  nanoparticles at different concentration and PBS for 24 h. After 24 h, 2', 7'-dichlorofluorescein diacetate (DCFH-DA) was added to each well and incubated for 30 min at  $37^\circ\text{C}$ . Finally, the fluorescence was detected by fluorescence microscope.

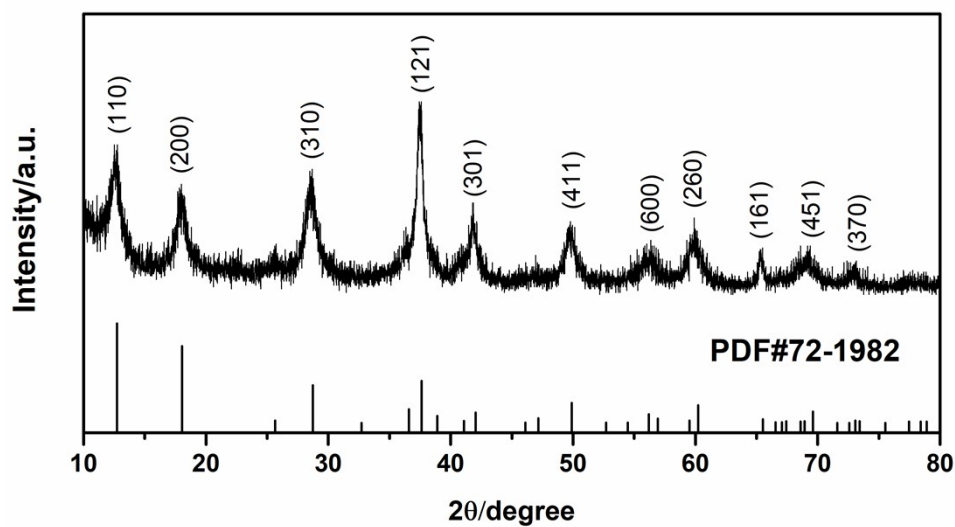
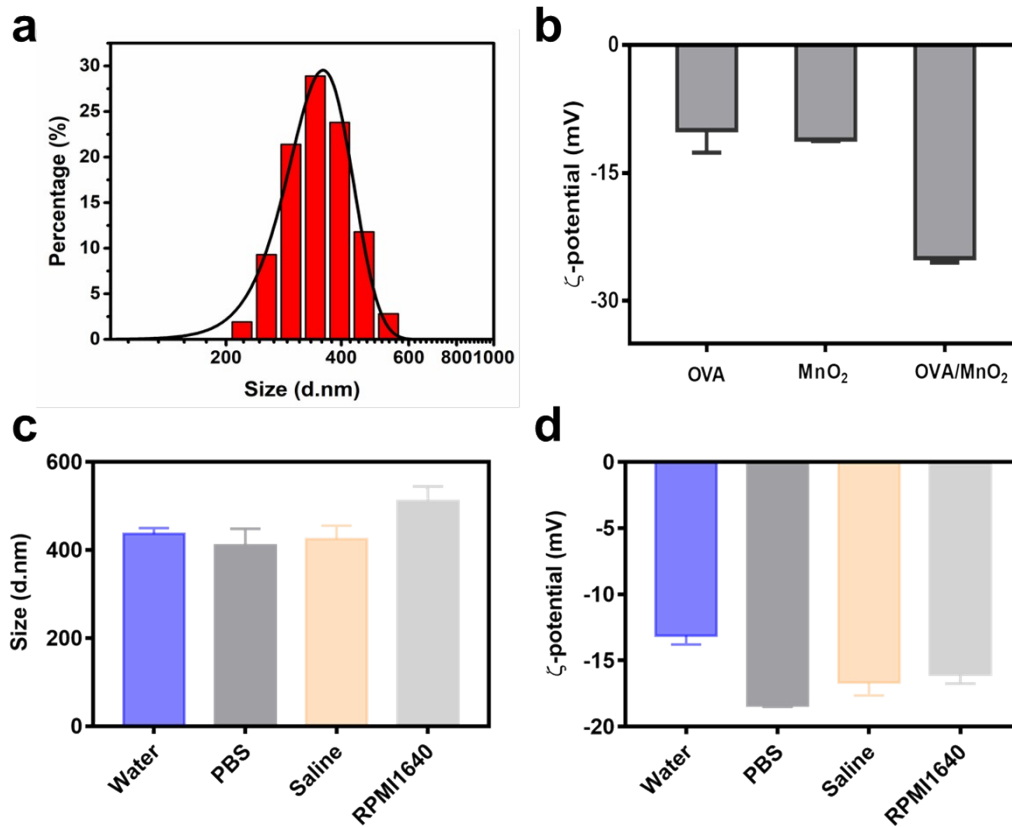
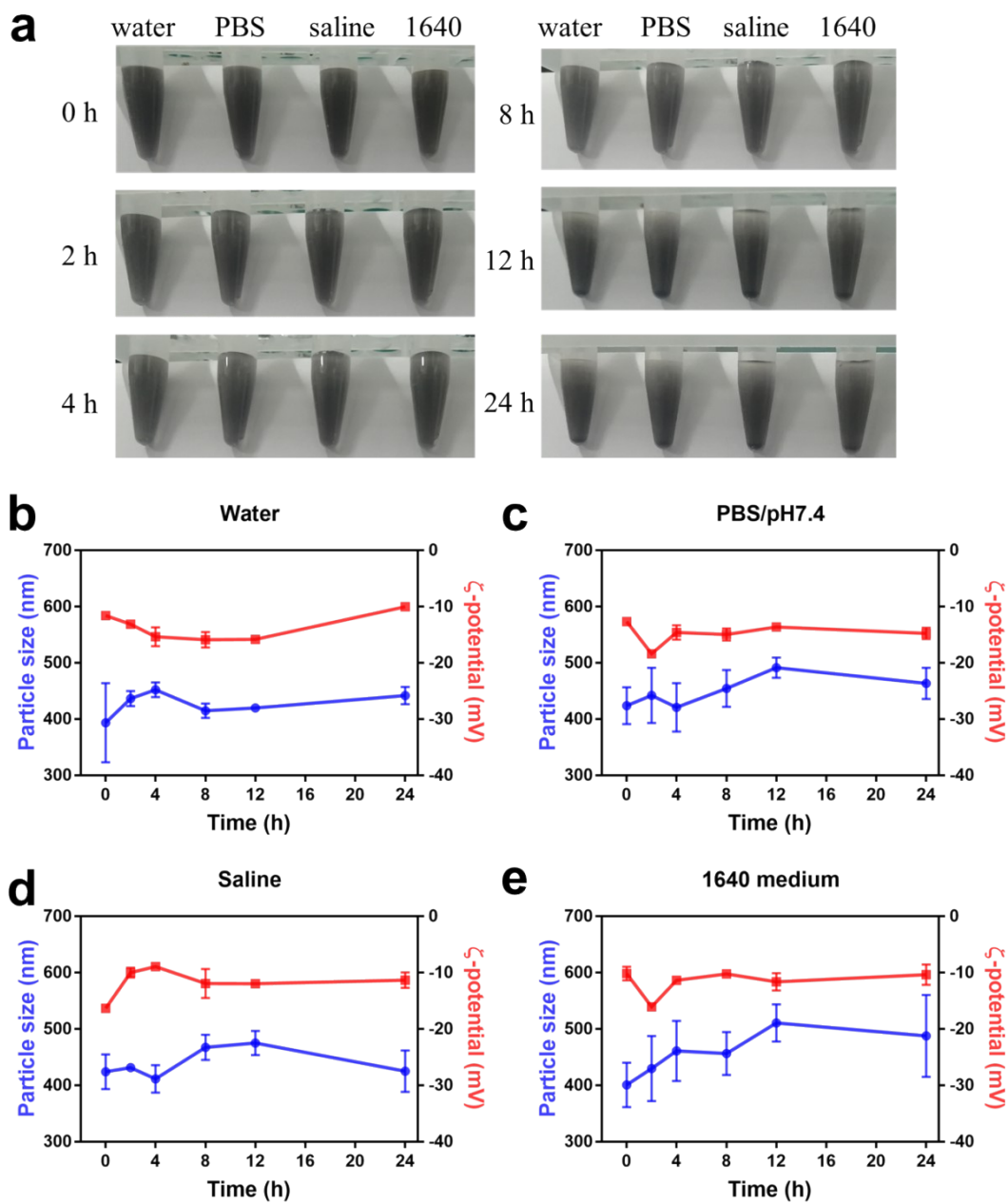


Figure S1. XRD spectrum of  $\text{MnO}_2$



**Figure S2.** (a) The size distribution of the MnO<sub>2</sub> nanoparticles. (b) Zeta potentials of OVA, MnO<sub>2</sub>, OVA/MnO<sub>2</sub> measured by dynamic light scattering (DLS). The average zeta potentials of OVA, MnO<sub>2</sub> and OVA/MnO<sub>2</sub> are -9.99, -11.1 and -25 mV, respectively. Compared with MnO<sub>2</sub>, the increase of OVA/MnO<sub>2</sub> is attributed to electronegativity of OVA, indicating successful OVA coating. (c) Particle size and zeta potential (e) of the MnO<sub>2</sub> nanoparticles in various solutions, including water, PBS, saline, RPMI1640 basal medium.



**Figure S3.** (a) Colloidal stability. (b-e) Size distribution and zeta potential changes of the MnO<sub>2</sub> nanoparticles in 24 h in (b) water; (c) PBS/pH7.4; (d) saline and (e) 1640 medium.

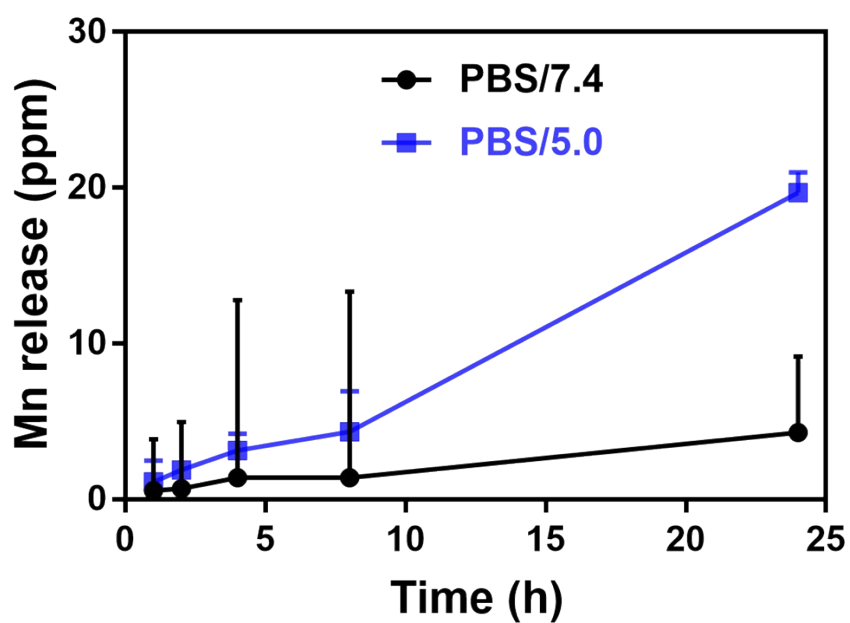


**Figure S4.** Mn ions release from the MnO<sub>2</sub> suspension (in phosphate buffer solution of pH7.4 or pH5.0) within 24 h.

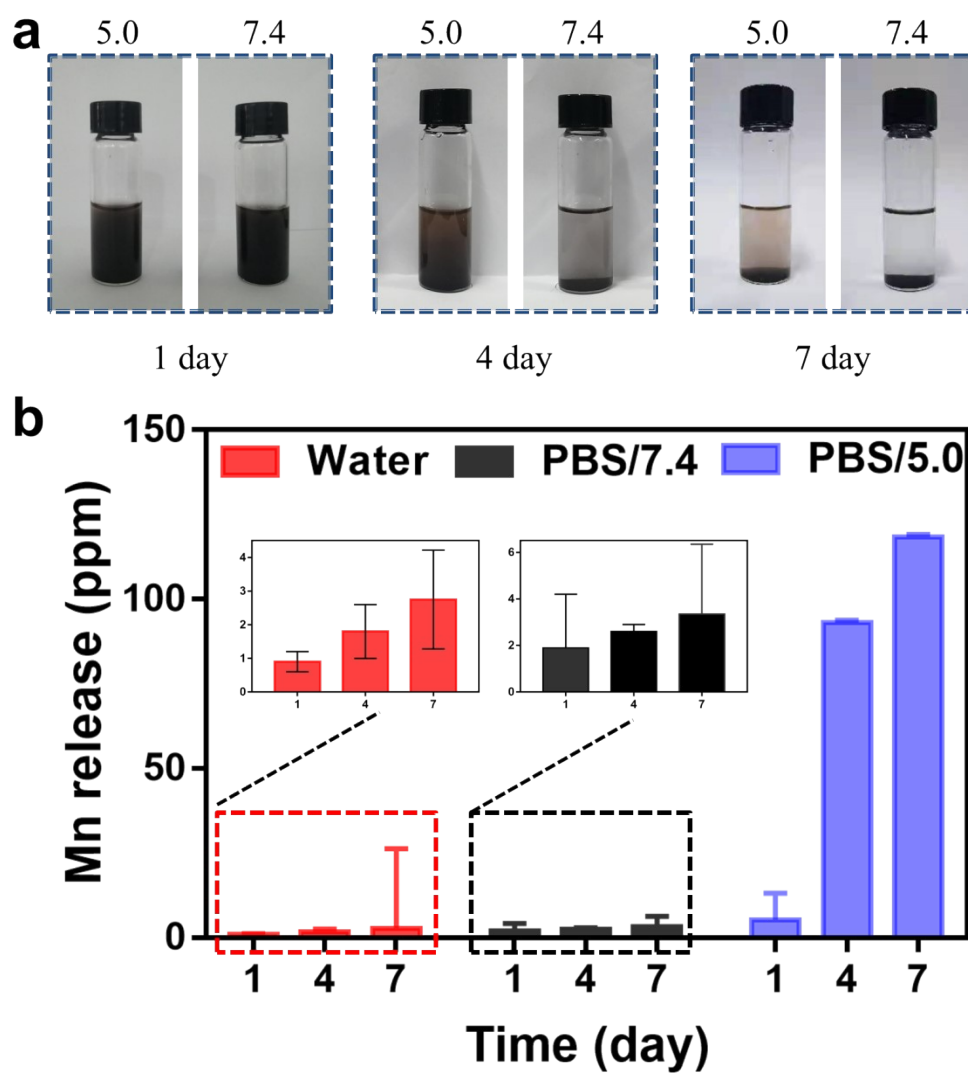


**Figure S5.** (a) Stability observation of the  $\text{MnO}_2$  at different pH values (5.0 and 7.4) over time. (b) Mn ions release from the  $\text{MnO}_2$  aqueous solution within 7 days.

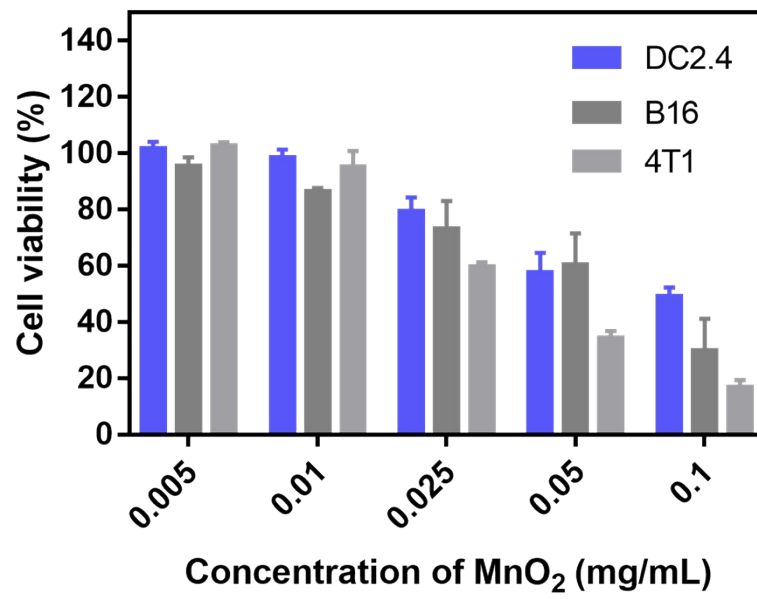


**Figure S6.** In vitro cytotoxicity of the MnO<sub>2</sub> nanoparticles in DC2.4, B16 and 4T1 cells.



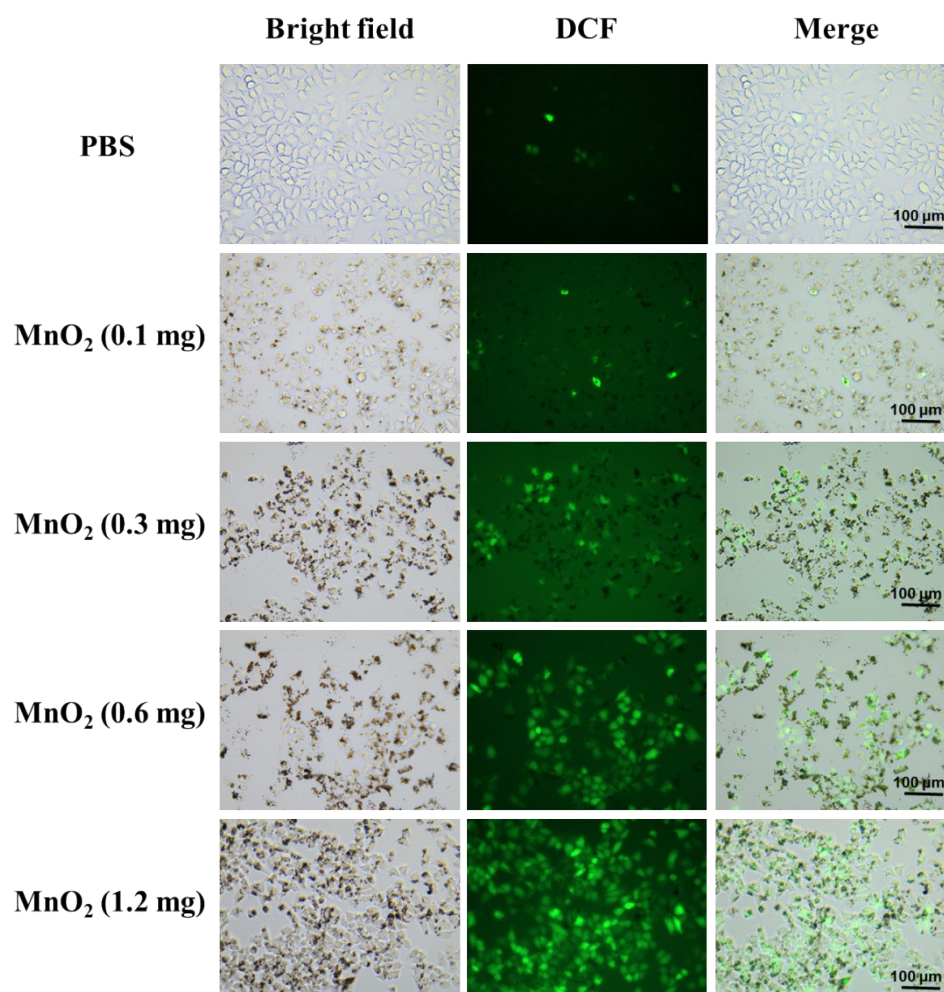


**Figure S7.** Intracellular HO· detections using DCFH-DA as a probe in different samples (PBS and MnO<sub>2</sub>). Each series can be classified into bright field, green fluorescence from DCF and merge, respectively. The enhanced green fluorescence from MnO<sub>2</sub>-treated group was observed in comparison with the control group.

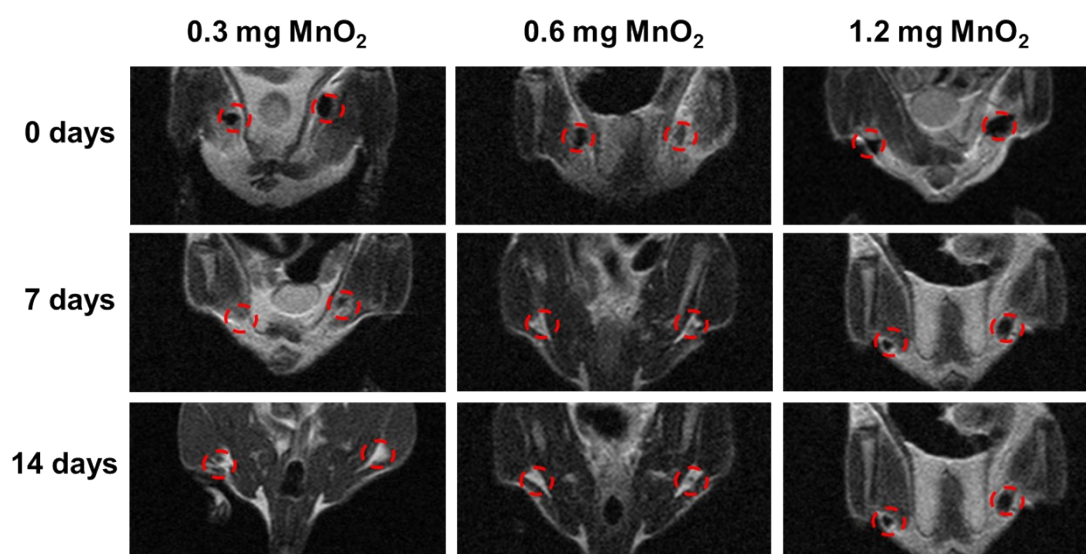


**Figure S8.** MRI of materials at different time points at the injection site of mice.

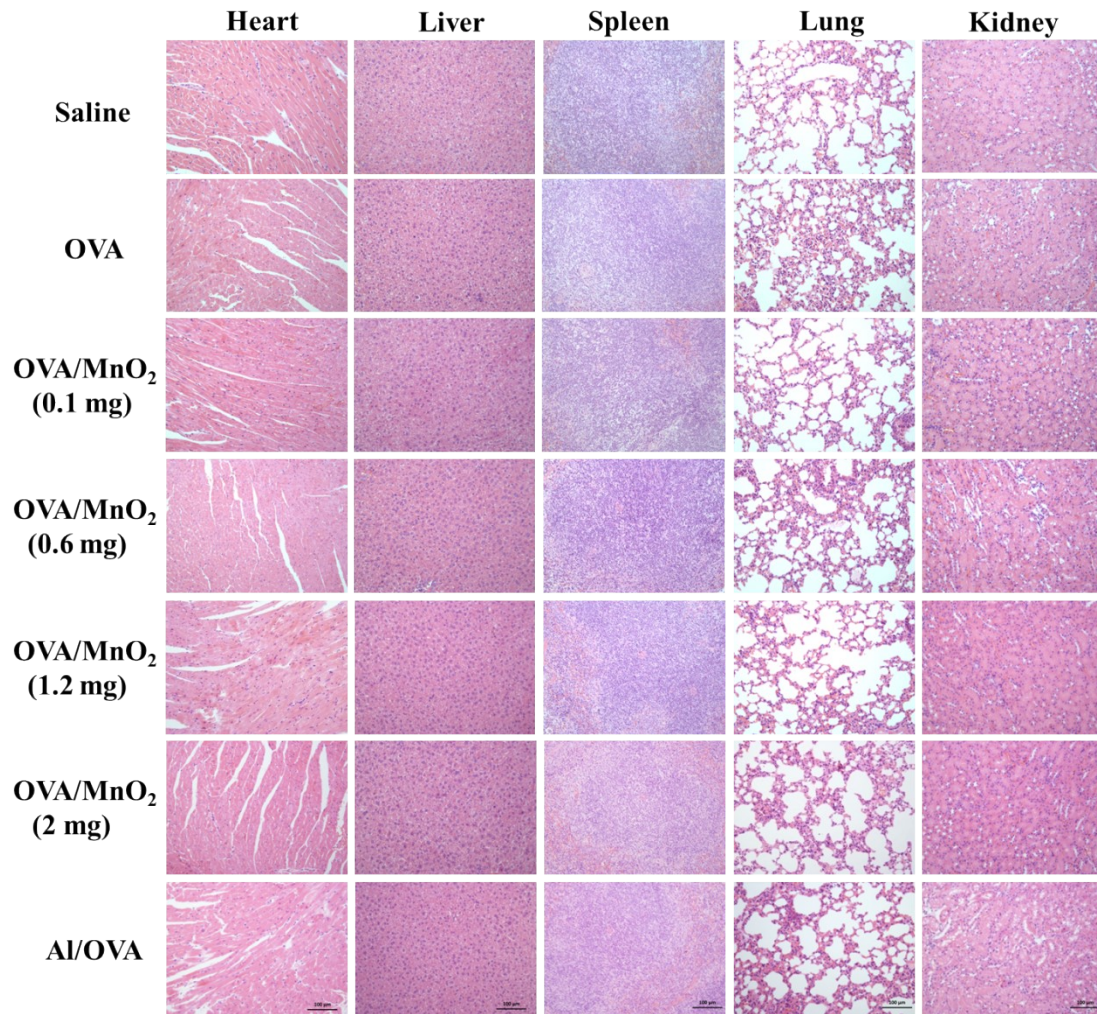


**Figure S9.** Evaluation of the biological safety of key organs (heart, liver, spleen, lung and kidney) after subcutaneous immunization with different vaccine formulations. Scale bar, 100  $\mu$ m.

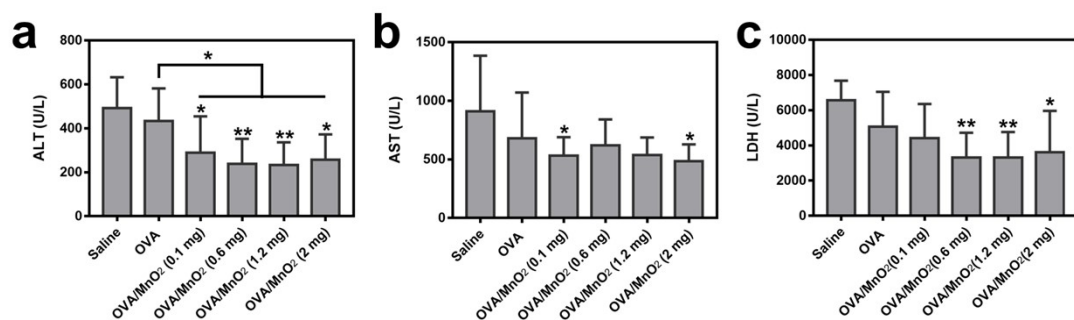


**Figure S10.** Serum of alanine transaminase (ALT), aspartate transaminase (AST), and lactate dehydrogenase (LDH) in mice measured at 23 d during the course of treatment. (\* $P < 0.05$ , \*\* $P < 0.01$ ;  $n = 5$ ).